

Chaos in Neuronal Networks with Balanced Excitatory and Inhibitory Activity

C. van Vreeswijk and H. Sompolinsky

Neurons in the cortex of behaving animals show temporally irregular spiking patterns. The origin of this irregularity and its implications for neural processing are unknown. The hypothesis that the temporal variability in the firing of a neuron results from an approximate balance between its excitatory and inhibitory inputs was investigated theoretically. Such a balance emerges naturally in large networks of excitatory and inhibitory neuronal populations that are sparsely connected by relatively strong synapses. The resulting state is characterized by strongly chaotic dynamics, even when the external inputs to the network are constant in time. Such a network exhibits a linear response, despite the highly nonlinear dynamics of single neurons, and reacts to changing external stimuli on time scales much smaller than the integration time constant of a single neuron.

a cell generated by the activity of its K presynaptic excitatory cells has a mean proportional to K and a relatively small fluctuating component proportional to \sqrt{K} (8). The same holds for the inhibitory input. Because we focus on the role of the network dynamics in generating the temporal irregularity, we assume that the external input does not fluctuate; thus, each cell receives a constant external excitatory input of order K . The mean synaptic inputs are also proportional to the firing rates of the presynaptic populations. Because the threshold is only of the order of \sqrt{K} synaptic inputs, the total synaptic input to a cell will be overwhelmingly depolarizing or hyperpolarizing unless the activity of the excitatory and inhibitory populations dynamically adjust

Recent theoretical and experimental studies have focused on the source of the temporally irregular firing patterns of neurons in cortex, as exemplified by their Poisson-like histograms of interspike intervals (1). Understanding the origin of this irregularity has important implications for elucidating the temporal components of the neuronal code in cortex. In experiments performed *in vitro*, cortical slices showed regular firing patterns when stimulated by a constant current, indicating that the irregular firing of neurons in the intact brain is due to strong temporal fluctuations in their synaptic inputs (2); however, the origin of the fluctuations of the synaptic inputs is not yet known. Furthermore, because a neuron in cortex makes thousands of synaptic contacts with other neurons, the fluctuations in the total synaptic input to a cell is expected to be relatively small even when individual synaptic inputs are strongly fluctuating (3). It was recently proposed that the timing of the firing of cells in cortex is sensitive to the relatively small fluctuations in their total synaptic input because the excitatory inputs are largely canceled by the inhibitory ones (4, 5). This intriguing hypothesis raises several questions about (i) the origin of the irregularity of individual synaptic inputs, (ii) the fine-tuning of synaptic constants required to ensure the balance between the total excitatory and inhibitory currents, and (iii) the functional benefits of generating synaptic currents that cancel each other. Several studies (5) have investigated the balance hypothesis in network models, but whether a balance between excitation and inhibition can emerge without fine-tuning of the network parameters remained an open question.

We studied a simple network of N_E excitatory and N_I inhibitory neurons. An ad-

ditional N_0 neurons from outside the network provide external excitatory inputs to the network neurons (Fig. 1). The model neurons are two-state units that update their state sequentially (6). The updated state of a neuron is active if the value of its input at the time of update exceeds its threshold; otherwise, it is quiescent. Biologically, the inputs to a unit correspond to the synaptic currents impinging on a neuron, and the time between two consecutive updates of a unit represents the neuronal membrane time constant (approximately 10 ms).

An important aspect of the architecture is the random, sparse connectivity. On average, K excitatory, K inhibitory, and K external neurons project to each neuron in the network. Although the average number of projections, K , is large, it is still much smaller than the total number of neurons in the subpopulations N_E and N_I . Also important is the assumption that the individual connections are relatively strong, namely, that only \sqrt{K} excitatory inputs are needed to cross the firing threshold (7). For example, each cell may receive about $K = 1000$ input currents, each on the order of 10.0 pA, and the threshold current may be about 0.3 nA. Because the number of inputs that are shared by two cells is relatively small, the firing patterns of pairs of neurons are only weakly correlated. Hence, the input to

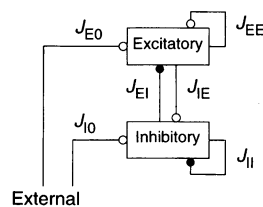


Fig. 1. Schematic representation of the network architecture. Excitatory connections between populations are shown as open circles; inhibitory ones, as filled circles.

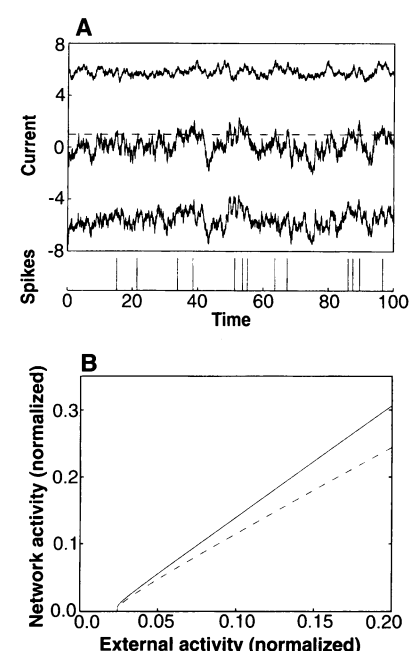


Fig. 2. (A) Temporal structure of the inputs and activity of a single excitatory unit. The upper panel shows the total excitatory input (consisting of external input and excitatory feedback) (upper trace) and the total inhibitory input (lower trace), as well as the net input (middle trace). The currents are shown in units of the threshold (dashed line). They were calculated by sampling from the Gaussian statistics of the currents predicted by the theory (8). Below, the times when the cell switched to the active state are indicated. The cell is set to the active state when a suprathreshold net input coincides with the update time of the cell (6). **(B)** The mean activity of the excitatory neurons (solid line) and the inhibitory ones (dashed line) as functions of the activity of the external units (10). The activities shown here and in the following figures correspond to firing rates divided by their maximum value. Assuming a neuronal maximum rate of 1000 Hz, a mean activity of 0.1 corresponds to a firing rate of 100 Hz. Parameter values: $K = 1000$, $J_{E0} = J_{EE} = J_{IE} = 1.0$, $J_{I0} = 0.8$, $J_{EI} = -2.0$, $J_{II} = -1.8$, $\theta_E = 1.0$, $\theta_I = 0.8$, and $D = 0.3$ in (A) and (B). Also in (A), $m_0 = 0.08$ and $\tau = 0.9$.

themselves so that the large total inhibitory input nearly cancels the large excitatory one (9). This balance between excitation and inhibition generates a net synaptic input whose mean and fluctuations are both on the order of the threshold. The precise timing of the crossing of the threshold is determined by the fluctuations of the synaptic input, yielding a strongly irregular pattern of activity (Fig. 2A). This disorder is a signature of deterministic chaos. Its presence does not require external sources of noise. One feature of the balanced network is that although the single-cell dynamics is highly nonlinear, the population-averaged rates increase nearly linearly with the external input (Fig. 2B). This linear dependence results from the adjustments of these rates to maintain the balance between the total excitatory and inhibitory inputs to the cells (10). Thus, the balance of the inhibition and excitation is an emergent property of the network dynamics and does not require precise tuning of the network parameters.

The balanced state is characterized also by a broad distribution of (time-averaged) firing rates across the network. This distribution is the outcome of the different synaptic projections on each neuron as well as their different threshold levels (7). Figure 3A shows the analytical results of the distribution of rates in the excitatory population for different values of mean rates. A prominent feature is the skewness of the distribution at low mean rates. Because in our model the temporal fluctuations are generated by the network activity itself, they are relatively small when the mean network activity is low. Hence, only those neurons that have relatively low thresholds fire vigorously; the rest show activity levels much lower than the mean rate. This feature agrees well with experimentally obtained histograms of firing rates of neurons in the monkey prefrontal cortex (Fig. 3B) (11). Our analysis shows that increasing the external inputs to the network shifts the peak of the distribution to larger values but does not give rise to a bimodal distribution (Fig. 3A).

Fig. 3. (A) The distribution of the rates of neurons in the excitatory population for different population-averaged rates: (solid line) $m_E = 0.01$ and (dashed line) $m_E = 0.03$. The rate distribution is shown in terms of the local rates divided by the mean rate. Parameters are as in Fig. 2B. **(B)** The distribution of firing rates of neurons in the right prefrontal cortex of a monkey attending to a variety of stimuli (light source and sound) and executing simple reaching movements (11). The rates were averaged over the duration of events (stimuli or movements) that showed a significant response. The average rate was 15.8 Hz. Most cells fire at a lower rate, whereas a small fraction of the cells fire at much higher rates.

One possible functional advantage of the balanced state is that the balanced network quickly tracks changes in the rate of the external input. The response time of the population rates is shorter than the time constant of single units by a factor of $1/\sqrt{K}$. An example of tracking a ramped external input $m_0(t) = m_0 + v_0 t$ is shown in Fig. 4. For comparison, we also show the slow response of an unbalanced network of linear units with the same stationary rates and the same single-unit time constants as our network (12). The ability of our network to react to changes in its environment on time scales that are much shorter than the update times of the individual neurons is a result of the combination of the large synaptic gain (on the order of \sqrt{K}) and the asynchronous nature of the dynamics. A change in the external input by a small amount over a small time increment generates a relatively large change in the synaptic inputs to the neurons in the network. As a result, those neurons that happen to be ready to update make a large change in their activity level. By successively recruiting different groups of neurons, the network population rates quickly adapt to the

changing input.

The chaotic nature of the balanced state is similar in many respects to the chaotic states of spin-glasses with random asymmetric connection matrices (13, 14). However, in spin-glasses, the balance between inhibition and excitation is automatically guaranteed for an arbitrary state of the network by the randomness of the signs of the connections. In the present networks, the sign of the connections is spatially organized, and the balance between excitation and inhibition is maintained by the network dynamics.

Cortical neurons and circuits are much more complex than the simple network we have studied here, but the mechanism proposed here can also account for the irregular spike trains observed in cortical cells. Indeed, the simplicity of our model suggests that irregular spiking is an emergent network property that does not necessarily depend on intricate cellular mechanisms. Other aspects of balanced networks such as broad, skewed rate distributions and fast tracking are expected to hold also for more realistic models. The linear response of population activities will also hold provided that synaptic inputs are summed approximately linearly. Finally, the predicted chaotic activity of the balanced networks puts constraints on the use of precise temporal patterns of firing as neural codes.

REFERENCES AND NOTES

- B. D. Burns and A. C. Webb, *Proc. R. Soc. London Ser. B* **194**, 211 (1976); R. J. Douglas and K. A. C. Martin, *Trends Neurosci.* **14**, 286 (1991); W. R. Softky and C. Koch, *J. Neurosci.* **13**, 334 (1993).
- G. R. Holt, W. R. Softky, C. Koch, R. J. Douglas, *J. Neurophysiol.* **75**, 1806 (1996); Z. F. Mainen and T. J. Sejnowski, *Science* **268**, 1503 (1995).
- The fluctuations in the total synaptic input can be large if the different individual inputs are strongly synchronized. Model networks with a high degree of connectivity can display chaotic states characterized by strongly synchronized bursts of activity (15). Whether cortical networks exhibit such spatially coherent bursts under normal conditions is questionable.
- M. N. Shadlen and W. T. Newsome, *Curr. Opin. Neurobiol.* **4**, 569 (1994); *ibid.* **5**, 248 (1995); W. R. Softky, *ibid.*, p. 239; A. Bell, Z. Mainen, M. Tsodyks, T. Sejnowski, *Soc. Neurosci. Abstr.* **20**, 1527 (1994).
- D. J. Amit and N. Brunel, *Cereb. Cortex*, in press; M. Tsodyks and T. Sejnowski, *Network (Bristol)* **6**, 111 (1995).
- The details of the dynamics are not essential. The simplest model for analytical study is one in which at each time step an updating neuron is chosen at random. Qualitatively similar behavior exists if the neurons are updated sequentially in a fixed order. Another possibility is a smooth dynamic model for analog units (13). These models differ primarily in the details of their short-time correlations. Time is scaled so that excitatory neurons are updated once per unit of time, and inhibitory units are updated every τ time units.
- The probability that a given excitatory (inhibitory) neuron projects to another given neuron is K/N_E (K/N_I). External neurons have a probability K/N_0 of connecting to a given cell in the network. All nonzero projections from cells of the k th population onto cells of the k th population have a strength J_{kk} . Here $k = 0, E$,

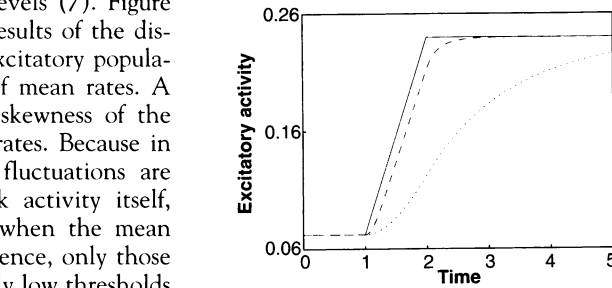
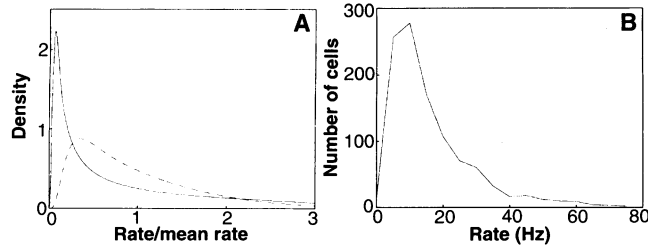


Fig. 4. The average excitatory rate (solid line) for an external drive that varies with time t . The external drive is constant at $m_0 = 0.06$ for $t < 1$, then increases linearly until $t = 2$, and thereafter remains constant at $m_0 = 0.16$. The dashed line shows the evolution of the excitatory rate for a hypothetical network that tracks the external rate infinitely quickly. The response of an unbalanced network of linear neurons is also shown (dotted line) (13). Parameters are the same as in Fig. 2A, except for m_0 .



I denote the external, excitatory, and inhibitory populations, respectively. Inhomogeneities are modeled by distributing the thresholds of population k uniformly between a minimum of $\theta_k \sqrt{K}$ and a maximum of $(\theta_k + D)\sqrt{K}$.

8. The total instantaneous input to a single neuron of population $k = E, I$ consists of weakly correlated fluctuating contributions. Therefore, we can assume, for large K , that it has Gaussian statistics with a mean given by

$$u_k(t) = K \sum_{i=0,E,I} J_{ki} m_i(t) \quad (1)$$

and variance

$$\sigma_k^2(t) = K \sum_{i=0,E,I} (J_{ki})^2 m_i(t) \quad (2)$$

The variable $0 \leq m_i(t) \leq 1$ denotes the unit activities averaged over all the units in the i th population. It represents the firing rate of the neuronal population relative to its maximal rate. A detailed analysis also yields the short-time correlations of the input, which decay on a time scale of order unity. The external input does not contribute to the fluctuations.

9. To ensure that the saturated states ($m_i = 1$ or 0) are not stable, the connection parameters J_{ki} must obey certain easily satisfied inequalities. They also ensure the existence of a balanced state. The stationary balanced state is stable provided that the inhibitory time constant τ is smaller than an upper bound τ_c . The value of τ_c typically ranges from 0.5 to 1.5.
10. In the balanced state, the means u_k (Eq. 1) are roughly equal to the population-averaged thresholds $\theta_k \sqrt{K}$, yielding for population activities m_E and m_I , the

following linear relation to the external activity m_0

$$m_0 = - \sum_{i=E,I} J_{ki}^{-1} (J_{i0} m_0 - K^{-1/2} \theta_i) \quad (3)$$

Here J^{-1} is the inverse of the 2×2 matrix of connections J_{ki} between the two network populations. The activities are thresholded to zero when the above relations yield negative values.

11. M. Abeles, H. Bergman, E. Vaadia, unpublished data.
 12. For comparison we consider a fully connected network of linear neurons where the coupling strengths between neurons in the network are equal to J_{ki}/K . These neurons integrate linearly their input with the same time constants as in the balanced network. The strengths of the synapses from cells outside of the network as well as the thresholds were chosen so that the stationary population rates of this network are the same as those for the balanced network.
 13. H. Sompolinsky, A. Crisanti, H. J. Sommers, *Phys. Rev. Lett.* **61**, 259 (1988).
 14. B. Derrida, E. Gardner, A. Zippelius, *Europhys. Lett.* **4**, 167 (1987). In this model, the randomness in the sign of the interactions is the result of the random nature of the embedded memories.
 15. D. Hansel and H. Sompolinsky, *Phys. Rev. Lett.* **68**, 718 (1992); *J. Comput. Neurosci.* **3**, 5 (1996); P. C. Bush and R. J. Douglas, *Neural Comput.* **3**, 19 (1991).
 16. We thank D. J. Amit, D. Hansel, and T. Sejnowski for extensive discussions. We are grateful to M. Abeles, H. Bergman, and E. Vaadia for permission to present their data.

11 June 1996; accepted 11 October 1996

Photolysis of the Carbon Monoxide Complex of Myoglobin: Nanosecond Time-Resolved Crystallography

Vukica Šrajer, Tsu-yi Teng, Thomas Ursby, Claude Pradervand, Zhong Ren, Shin-ichi Adachi, Wilfried Schildkamp, Dominique Bourgeois, Michael Wulff, Keith Moffat*

The biological activity of macromolecules is accompanied by rapid structural changes. The photosensitivity of the carbon monoxide complex of myoglobin was used at the European Synchrotron Radiation Facility to obtain pulsed, Laue x-ray diffraction data with nanosecond time resolution during the process of heme and protein relaxation after carbon monoxide photodissociation and during rebinding. These time-resolved experiments reveal the structures of myoglobin photoproducts, provide a structural foundation to spectroscopic results and molecular dynamics calculations, and demonstrate that time-resolved macromolecular crystallography can elucidate the structural bases of biochemical mechanisms on the nanosecond time scale.

Structural intermediates in biological reactions can be very short-lived, with lifetimes spanning the time scale from femtoseconds

V. Šrajer, T.-y. Teng, C. Pradervand, Z. Ren, W. Schildkamp, K. Moffat, Department of Biochemistry and Molecular Biology and the Consortium for Advanced Radiation Sources, The University of Chicago, Chicago, IL 60637, USA.

T. Ursby and M. Wulff, European Synchrotron Radiation Facility (ESRF), 38043 Grenoble Cedex, France.

S.-i. Adachi, Biophysical Chemistry Laboratory, Institute of Physical and Chemical Research, Saitama 351-01, Japan.

D. Bourgeois, UPR 9015/IBS, 38027 Grenoble, France, and ESRF, 38043 Grenoble Cedex, France.

*To whom correspondence should be addressed.

laser pulse. The results reveal directly the structural relaxation of the heme and protein in response to the ligand photodissociation and rebinding. The MbCO photolysis reaction has been studied in solution by numerous spectroscopic techniques (8–18) and computational approaches by molecular dynamics simulations (19–21), to which we relate our crystallographic results.

The nanosecond time-resolved crystallographic data were collected at the white beam station BL3 (ID9) at the European Synchrotron Radiation Facility (ESRF), Grenoble, France. Photolysis was initiated by 7.5-ns laser pulses, and subsequent structural changes were monitored with either a single 150-ps x-ray pulse or a 940-ns pulse train (22, 23). Photolysis and CO rebinding were also monitored optically (22). Complete x-ray data sets were obtained (Table 1) to 1.8 Å resolution at six time delays between laser and x-ray pulses: 4 ns (150-ps x-ray exposure, 15-mA beam current, single-bunch mode of operation of ESRF), 1 μs, 7.5 μs, 50.5 μs, 350 μs, and 1.9 ms (940-ns x-ray exposure, 150 mA, one-third filling mode).

Difference Fourier maps corresponding to each of the six time delays (Fig. 1, A to F) reveal the differences between the average structure at a time delay t , $\text{Mb}^*(t)$, with the stable MbCO structure. The MbCO content of the $\text{Mb}^*(t)$ state, which results from either incomplete initial photolysis or ligand recombination, cancels out in these maps. The reference map (Fig. 1G) displays the difference in electron density between the conventional, static structures of deoxy Mb (24) and MbCO (25). With the exception of the maps at time delays of 350 μs and 1.9 ms, all show a prominent negative feature (labeled P in Fig. 1, A to D and G) corresponding to loss of the CO upon photolysis. The peak value of this feature at the 4-ns time delay corresponds to -9.8σ where σ is the root-mean-square value of the difference electron density in the asymmetric unit. The magnitude of this feature declines with time as photodissociated CO recombines and, as expected, parallels the extent of recombination estimated from the time course of the optical signal (Fig. 2). That is, this feature carries information about ligand rebinding kinetics. The absence of features at longer time delays is also expected since optical data show that recombination of the photodissociated CO is complete by about 100 μs (Fig. 2). The longer time delay data therefore serve as negative controls to illustrate the complete optical and structural reversibility of the reaction. The initial fraction of photolyzed molecules is estimated to be $45 \pm 10\%$ from the initial amplitude of the optical change (22) and $42 \pm 10\%$ from comparison of the